International Journal of Greenhouse Gas Control xxx (2016) xxx–xxx

Contents lists available at ScienceDirect

International Journal of Greenhouse Gas Control

journal homepage: www.elsevier.com/locate/ijggc

Nesquehonite sequesters transition metals and CO_2 during accelerated carbon mineralisation

Jessica L. Hamilton[a,*], Siobhan A. Wilson[a], Bree Morgan[a], Connor C. Turvey[a], David J. Paterson[b], Colin MacRae[c], Jenine McCutcheon[d], Gordon Southam[d]

[a] School of Earth, Atmosphere and Environment, Monash University, Clayton, Melbourne, VIC 3800, Australia
[b] Australian Synchrotron, Clayton, Melbourne, VIC 3168, Australia
[c] CSIRO Mineral Resources, Clayton, Melbourne, VIC 3168, Australia
[d] School of Earth Sciences, The University of Queensland, St. Lucia, QLD 4072, Australia

ARTICLE INFO

Article history:
Received 29 August 2016
Received in revised form 24 October 2016
Accepted 5 November 2016
Available online xxx

Keywords:
Nesquehonite
Mineral carbonation
Carbon sequestration
Trace metals
Mg-carbonate minerals
Enhanced weathering
X-ray fluorescence microscopy

ABSTRACT

Acid leaching of ultramafic rocks to produce Mg^{2+}- and Ca^{2+}-rich solutions for mineral carbonation may inadvertently leach toxic trace metals. This study investigates the capacity of nesquehonite ($MgCO_3{\cdot}3H_2O$), a common product of mineral carbonation at Earth's surface conditions, to sorb Cr, Ni, Mn, Co and Cu from solution. Our results demonstrate that upon precipitation, nesquehonite rapidly sequesters transition metals present in solution at concentrations from 10 to 100 mg/L. Trace metal uptake appears to occur by substitution for Mg^{2+} in the nesquehonite crystal structure, and also by incorporation into minor, metal-rich phases, such as Fe-oxyhydroxides. This indicates that first row transition metals will likely be trapped and stored within Mg-carbonate minerals produced in industrial mineral carbonation reactors and in landscapes modified to capture atmospheric CO_2 via enhanced weathering. Thus, it is unlikely that trace metals will pose an environmental risk in the event of accidental release of wastewater.

1. Introduction

Anthropogenic carbon dioxide (CO_2) production is causing the concentration of atmospheric CO_2 to steadily increase, and is likely driving long-term changes to Earth's climate (IPCC, 2013). Consequently, there is a growing necessity to reduce or offset anthropogenic CO_2 emissions, and to develop lasting CO_2 storage solutions (IPCC, 2013). One emerging strategy, carbon mineralisation, enhances the natural process of silicate mineral weathering and CO_2 sequestration by precipitating environmentally benign Mg- and Ca-carbonate minerals (Lackner et al., 1995; Oelkers et al., 2008; Olajire, 2013; Power et al., 2013a; Seifritz, 1990). Importantly, this is the only CO_2 storage option that is considered permanent, given that carbonate minerals are known to persist at the Earth's surface on geological timescales (Lackner et al., 1995).

Carbon mineralisation under Earth's surface conditions is limited due to the slow dissolution kinetics of the silicate minerals which provide the cations necessary for carbonation. To address this issue, acid-leaching of ultramafic rocks and alkaline industrial wastes has been widely employed as a means of accelerating silicate mineral dissolution (*e.g.*, Maroto-Valer et al., 2005; McCutcheon et al., 2015; Park et al., 2003; Power et al., 2010; Teir et al., 2007b). Although enhanced weathering of these minerals (and associated sulfides and oxides) can provide a supply of Mg^{2+} and Ca^{2+} for carbonation to proceed, they also commonly contain low (<1 wt.%) but significant concentrations of first row transition metals (*e.g.*, Ni, Mn, Cr, Cu, Co) within their crystal structures (Kmetoni, 1984; Margiotta et al., 2012; Natali et al., 2013; Schreier, 1987; Seal et al., 2010; Wunsch et al., 2013). Most of these trace metals are toxic to biota at elevated concentrations and may be mobilised in the acidic solutions used for enhanced dissolution of waste rock or industrial wastes prior to mineral carbonation (Margiotta et al., 2012; Olsson et al., 2014b; Wunsch et al., 2013). Although it has been established that acid is neutralised during silicate mineral dissolution, the fate of mobilised trace metals during this process is an ecological concern that has not yet been adequately investigated (Marcon and Kaszuba, 2013; Olajire, 2013; Seal et al., 2010).

Production and release of metal-rich drainage during carbon mineralisation may cause both on-site and off-site contamination of surface waters, groundwater, soils, and sediments by a number of implementation scenarios, including *ex situ* processing plants,

* Corresponding author.
E-mail address: jessica.hamilton@monash.edu (J.L. Hamilton).

http://dx.doi.org/10.1016/j.ijggc.2016.11.006
1750-5836/

enhanced weathering of ultramafic wastes and landscapes, and *in situ* injection-based projects (Kirsch et al., 2014; Marcon and Kaszuba, 2013, 2015; Oelkers et al., 2008; Olsson et al., 2014a,b; Seal et al., 2010; Thomas et al., 2013; Wunsch et al., 2013). Proposed enhanced weathering schemes include the application of Mg-silicate minerals to natural landscapes, such as river catchments or coastal settings (Hartmann et al., 2013; Schuiling and de Boer, 2013), or the treatment of ultramafic mine tailings with sulfuric acid or acid generating sulfide minerals (McCutcheon et al., 2015, 2016; Power et al., 2010). In the case of landscape-scale geoengineering projects, containment or remediation of mobilised metals could be challenging and expensive due to their large spatial footprint. This concern is also relevant to *in situ* injection of CO_2 into basaltic or ultramafic rocks, given that dissolved CO_2 creates an initially acidic environment that could facilitate metal release (Flaathen and Gislason, 2007; Marcon and Kaszuba, 2013; Oelkers et al., 2008; Olsson et al., 2014b; Thomas et al., 2013; Wunsch et al., 2013). The trace metal composition of carbonate mineral products generated in *ex situ* mineral carbonation reactors may also influence their utility as value added products. Therefore, assessing and controlling the mobility of transition metals should be a key consideration during design and implementation of accelerated carbon mineralisation projects.

Mg-rich ultramafic minerals, favoured as feedstock for carbon mineralisation reactions, commonly weather to produce low-temperature hydrated magnesium carbonate minerals, such as nesquehonite ($MgCO_3{\cdot}3H_2O$) and hydromagnesite [$Mg_5(CO_3)_4(OH)_2{\cdot}4H_2O$] (Oelkers et al., 2008; Power et al., 2013b; Wilson et al., 2009). Nesquehonite is most readily formed at ambient temperatures and pressures at the Earth's surface, decomposing to more thermodynamically stable hydromagnesite over time, or at temperatures above 50 °C, depending on the environmental conditions (Davies and Bubela, 1973; Jauffret et al., 2015; Morgan et al., 2015). As a primary mineral product of carbon mineralisation reactions at Earth's surface, nesquehonite and other hydrated Mg-carbonate minerals may represent important, and previously unrecognised sinks for mobilised trace metals. The capacity of Mg-carbonate minerals to sorb potentially hazardous metals is fundamental to understanding and managing the potential environmental risk of metal release from accelerated carbonation reactions. To date, no other research has investigated the sorption of trace metals to hydrated Mg-carbonate minerals, including nesquehonite, which is the topic of this study.

Our experiments focus on uptake and immobilisation of the trace metals Ni^{2+}, Cr^{3+}, Mn^{2+}, Co^{2+} and Cu^{2+} under conditions relevant to low temperature carbon mineralisation. These transition metals were chosen because (1) they are commonly abundant in ultramafic rocks and industrial wastes; (2) they have the potential to substitute for Mg^{2+} within the crystal structures of minerals due to their similar ionic radii and charge; and (3) some of these elements can be highly toxic to aquatic life and humans when they exceed guideline limits (ANZECC and ARMCANZ, 2000). Given the mineralogy and aqueous conditions of these experiments, these findings could be applied to low temperature *ex situ* mineralisation of ultramafic minerals or alkaline industrial wastes, or enhanced weathering of ultramafic landscapes including mine waste stockpiles.

2. Materials and methods

2.1. Laboratory experiment: sorption of transition metals to nesquehonite

Nesquehonite was synthesised by mixing equal volumes (4.5 mL) of 1.8 M $MgCl_2{\cdot}6H_2O$ and 1.8 M K_2CO_3 (Robie and Hemingway, 1972), in the presence of transition metal solutions (1 mL). Transition metal (Ni, Cr, Mn, Co, Cu) stock solutions were prepared from hydrated divalent metal chloride salts. Trace metals were present at concentrations of 10 and 100 mg/L in parallel experiments. Cr was added in the soluble form of $CrCl_2$, and is expected to have rapidly oxidised in the stock solution to Cr^{3+}, the form commonly present in partially or fully serpentinised ultramafic rocks (Oze et al., 2007).

The $MgCl_2{\cdot}6H_2O$ reagent also contains significant Fe, confirmed by portable X-ray fluorescence (XRF) analysis (Olympus Delta 50 Premium Soil Exploration Analyzer DP4050). This was expected to allow the formation of Fe-bearing phases in these experiments. Because ultramafic rocks typically contain several wt.% of Fe, this allows for better comparison with carbon mineralisation reactions. ICP-MS analysis of starting reagents also reveals trace transition metal contamination in the initial Mg-chloride solution used for nesquehonite synthesis, including significant Cr (approximately 10% of total Cr in the 10 mg/L treatment, or 1% in the 100 mg/L treatment). Since identical volumes of Mg-chloride were added to all experiments, the concentrations of Cr contamination found in control treatments were used to normalise Cr concentrations across all other experiments. Higher levels of the added transition metal solutions provided elevated concentrations of trace metals for the experiments.

Previous studies have shown that when nesquehonite forms from a supersaturated solution, it initially precipitates as a gel-like colloidal suspension, with crystal size increasing over a period of hours to days (Cheng and Li, 2009). As such, two time treatments (5 min and 48 h) were used to assess the relative effectiveness of metal uptake between microcrystalline (5 min) and highly crystalline (48 h) nesquehonite.

The $MgCl_2{\cdot}6H_2O$ stock solution and the transition metal stocks were initially combined in experimental vials prior to the addition of the K_2CO_3 solution. Instantaneous formation of a fine-grained, white precipitate occurred upon addition of the K_2CO_3 solution. Air temperature and atmospheric relative humidity were 23 °C and 23%, respectively, at the beginning of the experiment. Following the 5 min and 48 h exposures to the trace metal solutions, the samples were centrifuged at 4000 rpm for 30 min. The supernatant from each vial was separated, syringe filtered (0.2 μm) and acidified to pH < 2 using double distilled HNO_3.

Each experiment was reproduced in triplicate and parallel control experiments were conducted with Milli-Q water (18.2 mΩ cm) substituted for trace metal reagents. All reagents were analytical grade and prepared in Milli-Q water. Glassware was soaked for a minimum of 24 h in 1 M HCl and thoroughly rinsed with Milli-Q water prior to use. Experiments were conducted in sterile, 10 mL polypropylene centrifuge vials.

We found that nesquehonite synthesised in the polypropylene vials typically did not form many large (i.e., millimetre-scale) crystals after 48 h; instead remaining as fine-grained (micrometre-scale) material. After centrifuging, the separated precipitate fractions were kept in sealed polypropylene vials for six days. They were then were emptied into petri dishes to air dry at the ambient temperature in our laboratory. A very small amount of solution remained in the vials, which caused larger crystals (>1 mm) of nesquehonite to develop in the six days between centrifuging and emptying vials into petri dishes. Although recrystallisation was observed, a negligible fraction of trace transition metals could have been derived from the small amount of solution remaining in the precipitate during drying. Oven drying was not used at this stage because it can induce decomposition of nesquehonite to less hydrous Mg-carbonate phases.

Two of every three solid phase replicates, and all aqueous solutions, were analysed for Cr, Ni, Mn, Co, and Cu concentrations using Inductively Coupled Plasma Mass Spectrometry (ICP-MS, Thermo

Please cite this article in press as: Hamilton, J.L., et al., Nesquehonite sequesters transition metals and CO_2 during accelerated carbon mineralisation. Int. J. Greenhouse Gas Control (2016), http://dx.doi.org/10.1016/j.ijggc.2016.11.006

Finnigan X series II, quadrupole) in the School of Earth, Atmosphere and Environment at Monash University. Detection limits were <0.7 ppb for all elements analysed. These precipitates were oven dried at 50 °C for 24 h, then ground with an agate mortar and pestle to homogenise. Precipitate subsamples were then dissolved using double distilled HNO_3, and all samples were diluted with Milli-Q water prior to analysis to bring them within the calibration range. ICP-MS count rates were externally standardised by means of calibration curves created using commercially available stock solutions, and drift corrections were applied using Sc as an internal standard. The instrument variability was <5%.

2.2. Precipitate mineralogy

Precipitate subsamples from each treatment were prepared for analysis using powder X-ray Diffraction (XRD). Data were collected using a Bruker D8 Focus X-ray diffractometer (School of Chemistry, Monash University) equipped with a scintillation detector. The fine-focus Cu X-ray tube was operated at 40 kV and 40 mA. Data were collected over 2–80° 2θ, with a step size of 0.02° 2θ and a count time of 2 s/step. Mineral phases were identified using the ICDD PDF-2 database and the DIFFRAC^{plus} EVA Version 2 software package (Bruker XAS). Predicted mineralogy based on the geochemical constraints of the system was also investigated using PHREEQC modelling (Interactive 3.0.6-7757) with the Pitzer database (Parkhurst and Appelo, 1999).

2.3. Trace metal distribution in the precipitate

Representative subsamples of precipitates were analysed using Scanning Electron Microscopy (SEM) and Energy Dispersive Spectroscopy (EDS). Fibroidal arrays of both large nesquehonite crystals and finely crystalline material from each experiment were mounted on aluminium stubs using adhesive carbon tabs and coated with platinum. Preliminary SEM imaging was performed using a PHILIPS (FEI) XL30 TMP Environmental Scanning Electron Microscope using a backscattered electron (BSE) detector at 20 kV at The University of Melbourne. Further BSE and secondary electron (SE) images and EDS data were collected using a JEOL 7001F Field Emission Gun Scanning Electron Microscope (FEG-SEM) in the Monash Centre for Electron Microscopy. Images and EDS data were collected using an accelerating voltage of 15–20 kV.

A JEOL 8500F-CL HyperProbe Field-Emission Gun Electron Probe Microanalyser (FEG-EPMA) at CSIRO Clayton was used to produce elemental and cathodoluminescence (CL) maps from polished cross sections through experimental precipitates mounted in epoxy blocks. Synthetic nesquehonite, precipitated for 48 h from solutions with 100 mg/L trace metals, was analysed for Cr, Ni, Mn, Co, or Cu as appropriate, as well as Mg, K and Cl. The spatial distribution of elements was analysed at 20 kV with a beam current of 40 nA. The defocused beam had a pixel size of 5 μm and a dwell time of 50 ms per pixel. X-rays were detected using wavelength dispersive spectrometry (WDS) and a LIFH crystal. The CL signal within the Mn-doped sample of synthetic nesquehonite was collected in a hyperspectral manner using an integrated spectrometer with optical response from 200 to 950 nm. CL peaks were identified using the luminescence database of MacRae and Wilson (2008) and fitted with a Gaussian peak using in-house software, Chimage (MacRae et al., 2013).

The surface of the cross sectioned epoxy block used for electron microprobe analysis was re-cut and polished to remove beam damage from EMPA before analysis using the X-ray Fluorescence Microscopy (XFM) beamline at the Australian Synchrotron. Unfortunately, the Co doped sample was destroyed during preparation, and therefore could not be analysed. XFM was conducted with an incident monochromatic X-ray beam of 18.5 keV focused to ~2.0 μm using Kirkpatrick-Baez mirrors. Elemental maps were collected using the Maia detector (Ryan et al., 2010, 2014) with a step size of 2 μm for the Cr-doped sample and 4 μm for the Ni-, Mn- and Cu-doped samples. A dwell time of 1.33 ms/pixel was used for all samples. Full spectrum data were processed using the GeoPIXE software program (Ryan, 2000). X-ray Absorption Near Edge Spectroscopy (XANES) was conducted over the energy range 5.96–6.12 keV for the Cr absorption edge in the Cr-doped sample. A step size of 2–5 μm and a dwell time of 4–10 ms were used. Spectra were extracted from regions of interest using GeoPIXE and compared to published standards from the literature (Berry and O'Neill, 2004; Low et al., 2015; Vogel et al., 2014).

In this study, 'sorption' is used to describe trace metal uptake by possible mechanisms including adsorption and absorption because, as a proof of concept experiment, detailed tracing of sorption mechanisms is outside the scope of this study. Methods for more precise determination of the mode of uptake are suggested in the Discussion (Section 4).

3. Results

3.1. Trace metal sorption to precipitate

The experimental results show that Cr, Ni, Mn, Co and Cu were rapidly (<35 min for 5 min treatment and centrifuging time) removed from solution in both the 10 and 100 mg/L treatments (SI Table S1). The pH of experimental solutions ranged from 8.42 to 9.14. ICP-MS results demonstrate that generally >99 wt.% of trace metals are found within the precipitates (median: 99.63 wt.%), with <3.6% variability between replicates (SI Table S1).

3.2. Precipitate mineralogy

Precipitates are predominantly composed of nesquehonite and sylvite (KCl), with baylissite [$K_2Mg(CO_3)_2{\cdot}4H_2O$] also present at trace abundances, as confirmed by XRD and SEM (SI Fig. S1). XFM also reveals distinct Fe-rich phases, likely Fe-oxyhydroxides, associated with nesquehonite crystals. The Fe-oxyhydroxide phases are present at low abundances («1 wt.%), which would make them difficult to detect from XRD patterns given the data acquisition parameters used in this study. PHREEQC simulations were used to predict that sylvite (a highly soluble evaporite mineral) was undersaturated in experimental solutions, which is consistent with it having formed during sample drying as a thin coating over nesquehonite crystals (SI Fig. S1a, b, d, and e). Rare, small spheres (30–60 μm) of another Mg-carbonate phase were also observed in association with nesquehonite fibres and have been tentatively identified as dypingite [$Mg_5(CO_3)_4(OH)_2{\cdot}5H_2O$] (SI Fig. S1f) based on known Mg-carbonate decomposition sequences and morphologies.

3.3. Trace metal distribution in nesquehonite

Data from SEM-EDS demonstrate that trace metals are associated with nesquehonite crystals, but were not observed in sylvite above the detection limits of EDS. Cross sections through arrays of nesquehonite fibres allow investigation of the trace metal distribution within crystals, and along the growth axis of the crystals. Electron microscopy reveals that, in general, Ni, Mn, and Cu are distributed relatively evenly within nesquehonite crystals (Fig. 1). However, in the Cr doped nesquehonite crystal, trace phases containing higher concentrations of Cr appear to align with the growth axis of the nesquehonite crystals (Fig. 1b). Similarly sized grains of trace phases containing higher trace metal concentrations are also observed in samples containing Ni, Mn and Cu (Fig. 1d, f, j). Concentration zoning of Co is observed within nesquehonite, with higher

Please cite this article in press as: Hamilton, J.L., et al., Nesquehonite sequesters transition metals and CO_2 during accelerated carbon mineralisation. Int. J. Greenhouse Gas Control (2016), http://dx.doi.org/10.1016/j.ijggc.2016.11.006

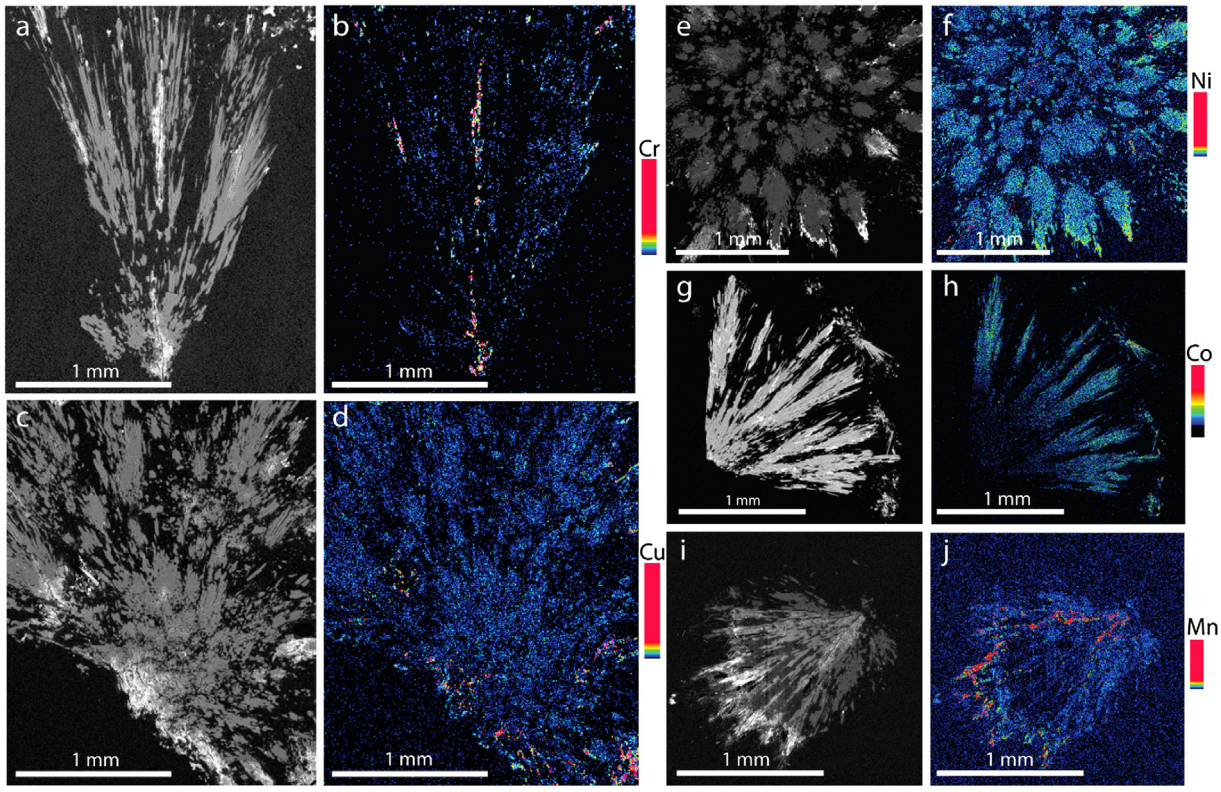

Fig. 1. BSE micrographs and EPMA maps (coloured) of cross sections through metal-doped nesquehonite crystals. BSE and EPMA data for samples of nesquehonite doped with Cr (a and b), Cu (c and d), Ni (e and f), Co (g and h), and Mn (i and j).

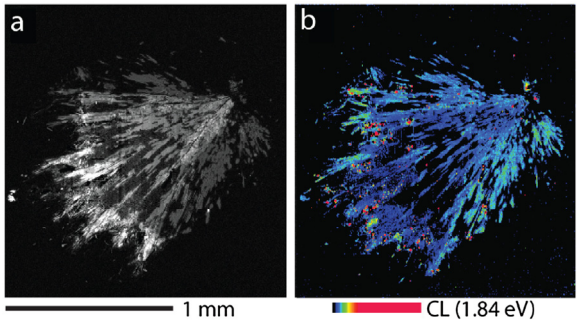

Fig. 2. (a) BSE micrograph of nesquehonite crystals containing Mn (Sample 48 h, 100 mg/L) with sylvite visible as a white precipitate on edges. Note that the darker region in the middle of the array of nesquehonite crystals is dominated by epoxy where the precipitate is not exposed at the surface. (b) Cathodoluminescence image generated by fitting the 1.84 eV peak clearly highlights nesquehonite grains indicating substitution of Mg^{2+} by Mn^{2+} within its crystal structure.

trace metal concentrations on the outer edges of the crystal array (Fig. 1h).

Cathodoluminesence spectroscopy along with the EPMA reveals a luminescence peak at 1.84 eV in the Mn-doped sample, which clearly illuminates the nesquehonite crystals in the sample (Fig. 2).

Synchrotron-based XFM data confirm the association of trace metals with the synthesised nesquehonite crystals (Fig. 3, SI Fig. S2–4). The regions mapped by EPMA that contain higher concentrations of trace metals are observed as chemically distinct minor (μm-scale) Fe-rich phases by XFM (Fig. 3, SI Fig. S2–4). XANES spectra show that Cr is dominantly present as Cr^{3+} in both the nesquehonite and the trace Fe-phases, with possible minor Cr^{6+} present in the Fe-bearing phase (SI Fig. S5).

4. Discussion

4.1. Immobilisation of trace metals by nesquehonite

Our combined ICP-MS, XRD, FEG-EPMA and XFM data show for the first time that trace metals (Cr, Ni, Mn, Co and Cu) are rapidly sorbed by Mg-carbonate minerals, such as nesquehonite, during simulated carbon mineralisation experiments. This finding confirms speculation by Olsson et al. (2014a,b) that trace metals may be sequestered by Mg-carbonate minerals (unspecified mineral species) forming in travertine deposits in the Semail Ophiolite in Oman and the Eyjafjallajökull volcano in Iceland, which have been studied as natural analogues for surface leakage of CO_2 as a result of injection into underground mafic to ultramafic rocks. Our observations are also supported by mass balance calculations made by Teir et al. (2007a) which indicate that Mn and Ni are present as impurities in hydromagnesite, and that Ni and Cu are found in Fe-oxide products, both of which were produced in a pH swing mineral carbonation experiment using serpentine feedstock.

Other common carbonate minerals, such as calcite ($CaCO_3$) and dolomite [$CaMg(CO_3)_2$] are known to be effective scavengers of alkaline earth and transition metals (such as Ba, Sr, Cd, Mn, Zn, Co and Ni) by surface adsorption, incorporation into the crystal structure by substitution for Ca or Mg, or as a co-precipitate (Calugaru et al., 2016; Wunsch et al., 2013; Zachara et al., 1991). However, until now, it was not known whether hydrated Mg-carbonate minerals could similarly sequester trace metals.

When supersaturated, nesquehonite is expected to initially precipitate as a gel-like colloidal suspension with crystal size increasing over a period of hours to days (Cheng and Li, 2009). However, we found that the growth of large, macroscopic crystals of nesquehonite was slower in the plastic centrifuge tubes than in the glass beakers used in preliminary experiments. It took

Please cite this article in press as: Hamilton, J.L., et al., Nesquehonite sequesters transition metals and CO_2 during accelerated carbon mineralisation. Int. J. Greenhouse Gas Control (2016), http://dx.doi.org/10.1016/j.ijggc.2016.11.006

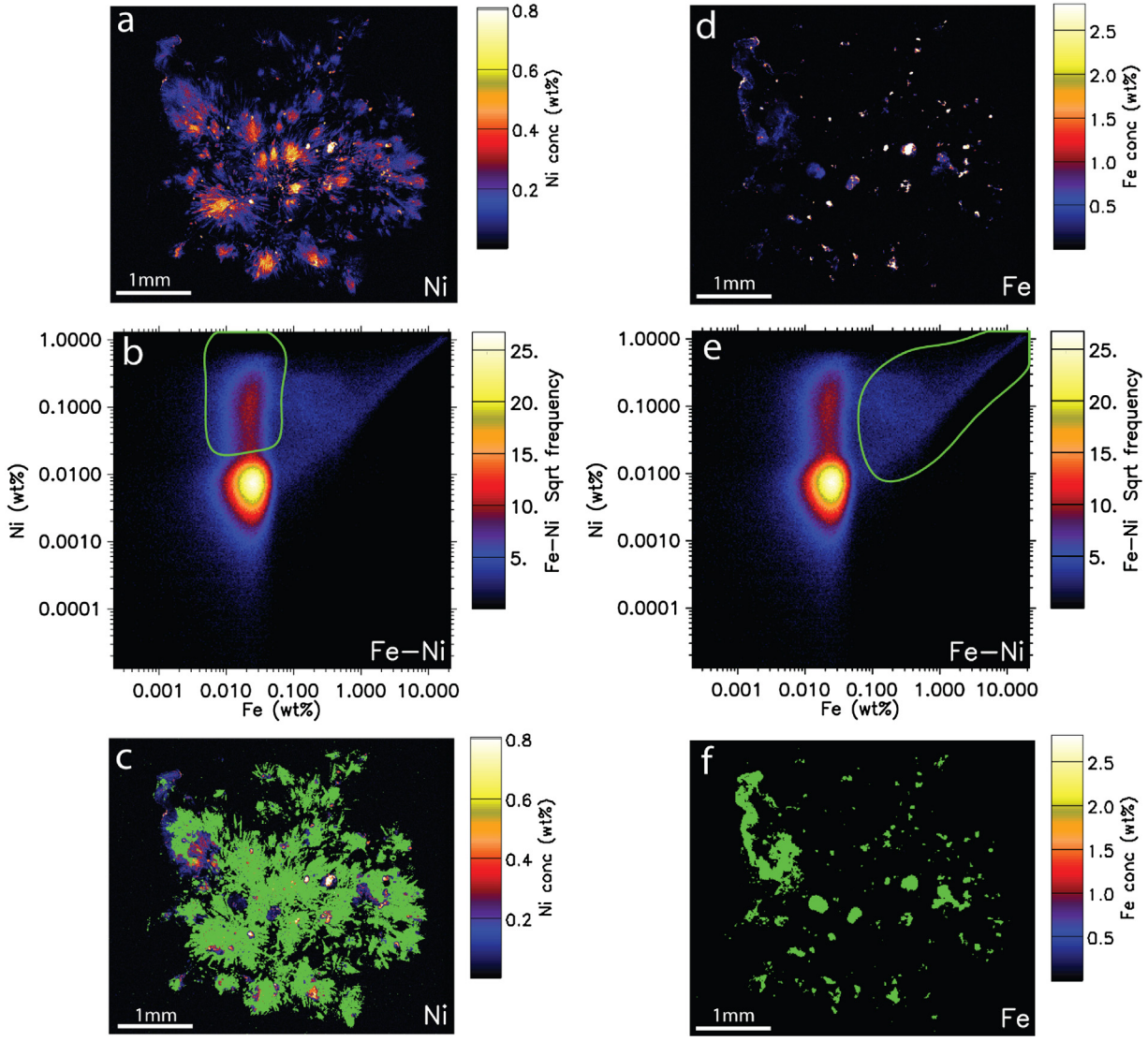

Fig. 3. Maps of spatial distribution of Ni highlight its association with nesquehonite and Fe-oxyhydroxides in the Ni-doped sample. (a) Synchrotron XFM map showing the distribution and concentration of Ni within the Ni-doped sample. (b) Ni *versus* Fe concentration plot, with region 1 (high Ni, low Fe) selected in the green field. (c) Region 1, highlighted in green on the Ni map, characterises Ni uptake in nesquehonite. (d) XFM image of contaminant Fe in the Ni doped sample. (e) Ni *versus* Fe concentration plot, with region 2 (high Ni, high Fe) selected in the green field. (f) Region 2 is highlighted in green on the Fe map and characterises Ni uptake in Fe-bearing trace phases. (For interpretation of the references to color in this figure legend, the reader is referred to the web version of this article.)

several days before large (>1 mm), well-ordered crystals formed in the residual material after centrifuging and removing most of the experimental solution. As such, while the initial precipitates formed after both time treatments were compositionally nesquehonite, they may have been structurally different. ICP-MS results from precipitate and supernatant samples (separated immediately after centrifuging) demonstrate that metal uptake is not limited by crystal size, and occurs instantaneously with formation of the nanoparticulate phase.

4.2. Mechanism for immobilisation

Substitution for Mg^{2+} appears to be the most likely mode of metal incorporation in nesquehonite, supported by mapping with EPMA (Fig. 1), CL spectroscopy (Fig. 2) and XFM (Fig. 3). The even distribution of trace metal concentration observed throughout nesquehonite in EPMA and XFM maps suggest that trace metals are incorporated into the crystal structure by substitution, rather than solely by adsorption to crystal surfaces, although the latter mechanism may play a role. CL spectroscopy provides compelling evidence that the relatively even distribution of Mn observed throughout the nesquehonite crystals represents crystallographic trapping via substitution for Mg^{2+}. The CL peak energy for the sample doped with Mn (1.84 eV), which illuminates the nesquehonite crystals, is a close analogy to the luminescence database energy for Mn^{2+} substitution in the Mg^{2+} site in dolomite (1.88 eV) and magnesite (1.82–1.9 eV) (MacRae and Wilson, 2008). Another potential contribution to this CL peak may be trace Fe in these precipitates, which is likely present as Fe^{3+} and can produce a CL peak at 1.71–1.91 eV in dolomite (MacRae and Wilson, 2008). However, XFM reveals Fe is approximately five times less abundant than Mn in the bulk nesquehonite crystal. As such, the peak at 1.84 eV is more likely to result from Mn^{2+} luminescence. The divalent transition metals tested (Ni^{2+}, Mn^{2+}, Co^{2+} and Cu^{2+}) have similar radii (<15% difference) and charge, are known to substitute for Ca^{2+} and Mg^{2+} in minerals such as calcite, dolomite and magnesite, and form carbonate mineral solid solutions (Comans and Middelburg, 1987; Franklin and Morse, 1983; Lumsden and Lloyd, 1984; Medlin, 1961;

Please cite this article in press as: Hamilton, J.L., et al., Nesquehonite sequesters transition metals and CO_2 during accelerated carbon mineralisation. Int. J. Greenhouse Gas Control (2016), http://dx.doi.org/10.1016/j.ijggc.2016.11.006

Prissok and Lehmann, 1986; Shannon, 1976; Zachara et al., 1991). As such, it is reasonable to predict that these cations substitute for Mg^{2+} in hydrated Mg-carbonates in the same way. This is supported by consistent observations of distribution for all trace metals tested, in EPMA and XFM maps (Fig. 2, SI Fig. S2–4). In these experiments, dopant trace metals were present in precipitates at an average of 680 mg/kg (100 mg/L experiments). This is within the capacity of carbonate minerals, such as calcite, to substitute these and similar trace metals (El Ali et al., 1993; Lamble et al., 1997). However, further X-ray Absorption Spectroscopy (XAS) work is required to definitively confirm the sorption mechanism (adsorption *versus* absorption).

The relatively even distributions of trace Fe (likely Fe^{3+}) and Cr^{3+} (as determined by XANES) within nesquehonite crystals also suggests substitution for Mg^{2+} (absorption), which is likely to be accommodated by coupled substitutions or the generation of structural defects. The possible contribution of Fe^{3+} to the detected Mn CL peak at 1.84 eV, and the known capacity for Fe^{3+} to substitute for Mg^{2+} in dolomite, support this conclusion (Papathanassiou, 2003; Prissok and Lehmann, 1986).

The toxicity of Cr is highly dependent on its oxidation state; Cr^{3+} is relatively immobile and environmentally benign, whereas Cr^{6+} is highly carcinogenic (drinking water limit <0.05 mg/L) (World Health Organisation, 2011). Leaching of Cr from ultramafic rocks by CO_2 rich fluids, and subsequent oxidation to toxic Cr^{6+}, represents a serious environmental concern (Natali et al., 2013). Because Cr^{3+} has a similar ionic radius and charge to Fe^{3+}, it is likely to be incorporated into hydrated Mg-carbonate minerals in a similar way. Cr is expected to have readily oxidised from Cr^{2+} in the soluble chloride salt to Cr^{3+} in the stock solution, and during our precipitation experiments may have undergone some precipitation of phases such as $Cr(OH)_3$ or $(Fe,Cr)(OH)_3$, which are relatively insoluble at neutral to alkaline pH (Kotaś and Stasicka, 2000; Rai et al., 1989). Despite this, Cr is observed to be distributed throughout nesquehonite crystals similarly to the divalent metals tested, and very little Cr is present in the oxidised form as Cr^{6+} (SI Fig. S5). Because the large crystals analysed by EMPA and XFM formed over a period of several days, this indicates nesquehonite may be an important sink for Cr because it can retain this transition metal even during recrystallisation of small crystals to macroscopic ones. However, in multi-metal experiments or natural systems, competitive sorption may affect the amount of Cr sequestered in mineral form and its retention during mineral recrystallisation and phase transitions. XFM data also reveal an association of Cr with trace Fe-oxyhydroxides, where it likely substitutes for Fe^{3+} (Schwertmann et al., 1989) within the crystal structure or adsorbs to crystal surfaces. It is possible that sequestration of Cr^{3+} in minerals such as nesquehonite or Fe-oxyhydroxides may limit oxidation to toxic Cr^{6+}; although dissolution of these phases, either by continued re-equilibration with a fluid or a change in environmental conditions, could remobilise Cr. Thus, ensuring long-term stability of Cr-bearing phases produced during accelerated carbon mineralisation is an important consideration.

Ni, Mn, Co and Cu were also associated with these Fe-oxyhydroxides, which have a high affinity for many trace metals (Manceau et al., 2000; Schwertmann et al., 1989; Trolard et al., 1995). This reveals there are multiple pathways for sequestration of potentially toxic transition metals in the carbonation products of ultramafic minerals and alkaline industrial waste materials.

4.3. Role of pH

The high alkalinity and pH of our experimental systems also has a key role to play in the immobilisation of trace metals during carbon mineralisation. At near neutral pH, transition metals are expected to be removed from solution by precipitation of hydroxides (Blowes et al., 2014; Lee et al., 2002). As such, the doped trace metals, and Fe in the system, could be expected to have precipitated here as Fe-oxyhydroxides and trace metal hydroxides, due to the low solubility of these metals at the neutral to alkaline pH conditions in the experimental vials. This likely occurred to some extent within the high-pH reagent stock solutions, before the experiments commenced. However, here we find the metals removed from solution are predominantly distributed within nesquehonite, as opposed to associated Fe-oxyhydroxides or other transition metal hydroxides, demonstrating that nesquehonite precipitation appears to be key to trapping metals under conditions relevant to carbon mineralisation.

The effect of pH on metal immobilisation in the context of carbon mineralisation has been demonstrated previously by Power et al. (2010) where Fe, Cu and Zn were immobilised during neutralisation of acidic leachate reacted with chrysotile [$Mg_3Si_2O_5(OH)_4$] mine tailings. In this system, the neutralisation reaction caused precipitation of the metals from solution and they were found to be associated with the formation of Fe-oxyhydroxides. Power et al. (2010) added pyrite (FeS_2) to treatments to provide a source of acidity, resulting in Fe-rich experiments with secondary precipitates dominated by Fe-oxyhydroxides; however, they do not report trace metal contents of any carbonate minerals that may have formed during these experiments. Rapid precipitation of Fe-oxide and Mg-carbonate minerals typically occurs after addition of a pH-raising additive in Mg-rich solutions, such as those leached from ultramafic minerals in carbonation reactors (Azdarpour et al., 2015; Park and Fan, 2004; Teir et al., 2007a). Our experimental results are applicable to this process, and indicate that first-row transition metals commonly released by leaching of ultramafic rocks will be incorporated into both Mg-carbonate and Fe-oxyhydroxide mineral products.

4.4. The fate of sorbed metals in nesquehonite

Our results demonstrate that nesquehonite is an effective crystallographic trap for transition metals, which may mean that this Mg-carbonate mineral can act as a relatively long-term and stable storage option. Although nesquehonite is the first Mg-carbonate mineral to precipitate at ambient temperatures, it typically decomposes into more stable, less hydrated phases over time, depending on environmental conditions (Ballirano et al., 2010, 2013; Davies and Bubela, 1973; Morgan et al., 2015; Schultz et al., 2014). It eventually decomposes to hydromagnesite, which can persist for millennia under neutral to alkaline conditions, and will ultimately form magnesite, which is a thermodynamically stable trap for CO_2 on timescales of millions of years (Ballirano et al., 2010, 2013; Davies and Bubela, 1973; Königsberger et al., 1999; Power et al., 2009; Wilson et al., 2006). The fate of sorbed metals during these phase transformations is an important consideration that remains to be determined.

Our experiments indicate that nesquehonite initially precipitated as a colloidal suspension. This is common for carbonate minerals, where crystal growth typically occurs via initial precipitation of an amorphous precursor phase, prior to the formation of a stable phase (Rodriguez-Navarro and Ruiz-Agudo, 2012). Because a small fraction of residual solution could not be removed from the precipitates by centrifuging, larger crystals were able to form in the solid phase over a period of several days. Crystal growth is likely to have occurred by dissolution–precipitation reactions, or by oriented attachment and aggregation of mineral nanoparticles (Rodriguez-Navarro and Ruiz-Agudo, 2012; Schultz et al., 2014). This may be responsible for the observed alignment of trace Fe-oxyhydroxides along large nesquehonite crystals in the Cr-doped sample (Fig. 1b). Also, the observed zoning of Co in the Co-doped nesquehonite crystal (Fig. 1h) could be explained if

Please cite this article in press as: Hamilton, J.L., et al., Nesquehonite sequesters transition metals and CO_2 during accelerated carbon mineralisation. Int. J. Greenhouse Gas Control (2016), http://dx.doi.org/10.1016/j.ijggc.2016.11.006

dissolution–precipitation reactions were occurring to form large crystals. For instance, if preferential incorporation of Mg during reprecipitation of larger crystals was followed by relative enrichment of the surrounding fluid in the trace metal dopant, this might allow greater Co sorption on the outer parts of the growing crystal. These findings are supported by observations that both Mg-carbonate and Fe-oxyhydroxide minerals continuously undergo dissolution-precipitation and re-equilibration reactions when in contact with a solution or humidity (Handler et al., 2014; Mavromatis et al., 2015; Morgan et al., 2015). Whether trace metals are retained during this process, or remobilised, is vital to understanding their longer-term behaviour in the environment. These experiments simulate diagenetic processes involving initial microcrystalline mineral precipitation, followed by a period of recrystallisation or aggregation into larger crystals over several days. Our observations suggest that trace metals will likely be reincorporated into the recrystallised Mg-carbonate phase, at least under the conditions of these experiments. It would be valuable to investigate whether there is any exchange of trace metals amongst Mg-carbonate minerals, Fe-oxyhydroxide minerals, and the fluid phase over time, especially during carbonate mineral phase transformations.

Trace metals associated with either hydrated Mg-carbonate or Fe-oxyhydroxide minerals may also be susceptible to remobilisation if environmental conditions were to change; for example if they were, respectively (1) exposed to acidic solutions, in which case the carbonate minerals can dissolve, or (2) covered with water or organic material, which may promote reductive mineral dissolution and trace metal release (Königsberger et al., 1999; Ribet et al., 1995). To prevent trace metal remobilisation from accelerated carbon mineralisation projects, the environmental conditions of stockpiled mineral products may need to be managed.

4.5. Future research

This study demonstrates that Mg-carbonate and Fe-oxyhydroxide minerals have the capacity to take up transition metals that are common in ultramafic rocks, likely by substitution for Mg^{2+} in the case of Mg-carbonate minerals. The precise mechanisms of sorption, the relative roles of adsorption and absorption, and the specific surface and crystal structure sites for metal uptake could be determined using Extended X-ray Absorption Fine Structure (EXAFS) spectroscopy, as in Frierdich and Catalano (2012) and Massey et al. (2014).

The capacity of nesquehonite to store transition metals (Cr, Ni, Mn, Co, Cu) may also have implications for the use of Mg-carbonate by-products of carbon mineralisation. Mg-carbonate minerals are currently utilised in a number of industrial applications including as raw material for production of magnesia and fire retardants, as rubber-strengthening agents and ingredients in pharmaceutical products (Hollingbery and Hull, 2010; Shan et al., 2012). The Carbon Capture Utilisation and Storage (CCUS) community has suggested that Mg-carbonates could find additional uses as construction materials, which may help to offset the costs of mineral carbonation projects (Galvez-Martos et al., 2016; Glasser et al., 2016; Olajire, 2013). If carbonation of ultramafic rocks or industrial wastes were implemented on an industrial scale, the capacity of mineral products to sequester potentially hazardous transition metals may be an important consideration for assessing their suitability for use in some industries. On the other hand, the use of nesquehonite precipitation may also have potential applications in environmental remediation of toxic transition metals.

Further research should investigate the possible risk of metal remobilisation from hydrated Mg-carbonate and Fe-oxyhydroxide phases that form during carbon mineralisation reactions, although sorption should be stable under oxidised and neutral to alkaline conditions. Another important avenue to explore will be whether trace metals remain sequestered within the crystal structures of Mg-carbonate minerals during decomposition of nesquehonite to hydromagnesite and ultimately to magnesite.

Acknowledgments

Funding for this work was provided by Carbon Management Canada and the NSW Department of Industry through grants awarded to S.A.W. and G.S. We acknowledge Massimo Raveggi for assistance with ICP-MS. Part of this research was undertaken on the X-ray Fluorescence Microscopy beamline at the Australian Synchrotron, Victoria, Australia (AS152/XFM/9393). This work was also supported by the Multi-modal Australian ScienceS Imaging and Visualisation Environment (MASSIVE) (www.massive.org.au).

Appendix A. Supplementary data

Supplementary data associated with this article can be found, in the online version, at http://dx.doi.org/10.1016/j.ijggc.2016.11.006.

References

ANZECC (Australian and New Zealand Environment and Conservation Council) and ARMCANZ (Agriculture and Resource Management Council of Australia and New Zealand), 2000. Australian and New Zealand Guidelines for Fresh and Marine Water Quality. National Water Quality Management Strategy Paper No. 4 Volume 1.

Azdarpour, A., Asadullah, M., Mohammadian, E., Hamidi, H., Junin, R., Karaei, M.A., 2015. A review on carbon dioxide mineral carbonation through pH-swing process. Chem. Eng. J. 279, 615–630.

Ballirano, P., De Vito, C., Ferrini, V., Mignardi, S., 2010. The thermal behaviour and structural stability of nesquehonite, $MgCO_3{\cdot}3H_2O$, evaluated by in situ laboratory parallel-beam X-ray powder diffraction: new constraints on CO_2 sequestration within minerals. J. Hazard. Mater. 178, 522–528.

Ballirano, P., De Vito, C., Mignardi, S., Ferrini, V., 2013. Phase transitions in the Mg-CO_2-H_2O system and the thermal decomposition of dypingite, $Mg_5(CO_3)_4(OH)_2{\cdot}5H_2O$: implications for geosequestration of carbon dioxide. Chem. Geol. 340, 59–67.

Berry, A.J., O'Neill, H.S.C., 2004. A XANES determination of the oxidation state of chromium in silicate glasses. Am. Mineral. 89, 790–798.

Blowes, D.W., Ptacek, C.J., Jambor, J.L., Weisener, C.G., Paktunc, D., Gould, W.D., Johnson, D.B., 2014. Chapter 11.5—the geochemistry of Acid Mine Drainage. In: Turekian, H.D.H.K. (Ed.), Treatise on Geochemistry. , second edition. Elsevier, Oxford, pp. 131–190.

Calugaru, I.L., Neculita, C.M., Genty, T., Bussière, B., Potvin, R., 2016. Performance of thermally activated dolomite for the treatment of Ni and Zn in contaminated neutral drainage. J. Hazard. Mater. 310, 48–55.

Cheng, W., Li, Z., 2009. Precipitation of nesquehonite from homogeneous supersaturated solutions. Cryst. Res. Technol. 44, 937–947.

Comans, R.N.J., Middelburg, J.J., 1987. Sorption of trace metals on calcite: applicability of the surface precipitation model. Geochim. Cosmochim. Acta 51, 2587–2591.

Davies, P.J., Bubela, B., 1973. The transformation of nesquehonite into hydromagnesite. Chem. Geol. 12, 289–300.

El Ali, A., Barbin, V., Calas, G., Cervelle, B., Ramseyer, K., Bouroulec, J., 1993. Mn^{2+}-activated luminescence in dolomite, calcite and magnesite: quantitative determination of manganese and site distribution by EPR and CL spectroscopy. Chem. Geol. 104, 189–202.

Flaathen, T., Gislason, S., 2007. The groundwater beneath Hekla Volcano, Iceland: a natural analogue for CO_2 sequestration. Geochim. Cosmochim. Acta 71, A283.

Franklin, M.L., Morse, J.W., 1983. The interaction of manganese(II) with the surface of calcite in dilute solutions and seawater. Mar. Chem. 12, 241–254.

Frierdich, A.J., Catalano, J.G., 2012. Distribution and speciation of trace elements in iron and manganese oxide cave deposits. Geochim. Cosmochim. Acta 91, 240–253.

Galvez-Martos, J.L., Morrison, J., Jauffret, G., Elsarrag, E., AlHorr, Y., Imbabi, M.S., Glasser, F.P., 2016. Environmental assessment of aqueous alkaline absorption of carbon dioxide and its use to produce a construction material. Resour. Conserv. Recycl. 107, 129–141.

Glasser, F.P., Jauffret, G., Morrison, J., Galvez-Martos, J.-L., Patterson, N., Imbabi, M.S.-E., 2016. Sequestering CO_2 by mineralisation into useful nesquehonite-based products. Front. Energy Res. 4.

Handler, R.M., Frierdich, A.J., Johnson, C.M., Rosso, K.M., Beard, B.L., Wang, C., Latta, D.E., Neumann, A., Pasakarnis, T., Premaratne, W., 2014. Fe (II)-catalyzed recrystallization of goethite revisited. Environ. Sci. Technol. 48, 11302–11311.

Hartmann, J., West, A.J., Renforth, P., Köhler, P., De La Rocha, C.L., Wolf-Gladrow, D.A., Dürr, H.H., Scheffran, J., 2013. Enhanced chemical weathering as a

geoengineering strategy to reduce atmospheric carbon dioxide, supply nutrients, and mitigate ocean acidification. Rev. Geophys. 51, 113–149.
Hollingbery, L.A., Hull, T.R., 2010. The thermal decomposition of huntite and hydromagnesite—a review. Thermochim. Acta 509, 1–11.
IPCC, 2013: Climate Change 2013: The Physical Science Basis. Contribution of Working Group I to the Fifth Assessment Report of the Intergovernmental Panel on Climate Change [Stocker, T.F., D. Qin, G.-K. Plattner, M. Tignor, S.K. Allen, J. Boschung, A. Nauels, Y. Xia, V. Bex and P.M. Midgley (eds.)]. Cambridge University Press, Cambridge, United Kingdom and New York, NY, USA, 1535 pp.
Jauffret, G., Morrison, J., Glasser, F.P., 2015. On the thermal decomposition of nesquehonite. J. Therm. Anal. Calorim. 122, 601–609.
Königsberger, E., Königsberger, L.-C., Gamsjäger, H., 1999. Low-temperature thermodynamic model for the system Na_2CO_3-$MgCO_3$-$CaCO_3$-H_2O. Geochim. Cosmochim. Acta 63, 3105–3119.
Kirsch, K., Navarre-Sitchler, A.K., Wunsch, A., McCray, J.E., 2014. Metal release from sandstones under experimentally and numerically simulated CO_2 leakage conditions. Environ. Sci. Technol. 48, 1436–1442.
Kmetoni, J., 1984. Woodsreef Mill Tailings—Investigation of Potental for Further Utilization as a Mineral Resource (Stage 1—Mineralogical Composition). Department of Mineral Resources, New South Wales, Report No. 84/11.
Kotaś, J., Stasicka, Z., 2000. Chromium occurrence in the environment and methods of its speciation. Environ. Pollut. 107, 263–283.
Lackner, K.S., Wendt, C.H., Butt, D.P., Joyce, E.L.J., Sharp, D.H., 1995. Carbon dioxide disposal in carbonate minerals. Energy 20, 1153–1170.
Lamble, G., Reeder, R., Northrup, P., 1997. Characterization of heavy metal incorporation in calcite by XAFS spectroscopy. Le Journal de Physique IV (7), C2-793–C792-797.
Lee, G., Bigham, J.M., Faure, G., 2002. Removal of trace metals by coprecipitation with Fe, Al and Mn from natural waters contaminated with acid mine drainage in the Ducktown Mining District, Tennessee. Appl. Geochem. 17, 569–581.
Low, F., Kimpton, J., Wilson, S.A., Zhang, L., 2015. Chromium reaction mechanisms for speciation using synchrotron in-situ high-temperature X-ray diffraction. Environ. Sci. Technol. 49, 8246–8253.
Lumsden, D.N., Lloyd, R.V., 1984. Mn(II) partitioning between calcium and magnesium sites in studies of dolomite origin. Geochim. Cosmochim. Acta 48, 1861–1865.
MacRae, C., Wilson, N.C., 2008. Luminescence database I—minerals and materials. Microsc. Microanal. 14, 184–204.
MacRae, C., Wilson, N.C., Torpy, A., 2013. Hyperspectral cathodoluminescence. Mineral. Petrol. 107, 429–440.
Manceau, A., Schlegel, M.L., Musso, M., Sole, V.A., Gauthier, C., Petit, P.E., Trolard, F., 2000. Crystal chemistry of trace elements in natural and synthetic goethite. Geochim. Cosmochim. Acta 64, 3643–3661.
Marcon, V., Kaszuba, J., 2013. Trace metal mobilization in an experimental carbon sequestration scenario. Procedia Earth Planet. Sci. 7, 554–557.
Marcon, V., Kaszuba, J.P., 2015. Carbon dioxide–brine–rock interactions in a carbonate reservoir capped by shale: experimental insights regarding the evolution of trace metals. Geochim. Cosmochim. Acta 168, 22–42.
Margiotta, S., Mongelli, G., Summa, V., Paternoster, M., Fiore, S., 2012. Trace element distribution and Cr(VI) speciation in Ca-HCO_3 and Mg-HCO_3 spring waters from the northern sector of the Pollino massif, southern Italy. J. Geochem. Explor. 115, 1–12.
Maroto-Valer, M.M., Fauth, D.J., Kuchta, M.E., Zhang, Y., Andrésen, J.M., 2005. Activation of magnesium rich minerals as carbonation feedstock materials for CO_2 sequestration. Fuel Process. Technol. 86, 1627–1645.
Massey, M.S., Lezama-Pacheco, J.S., Nelson, J.M., Fendorf, S., Maher, K., 2014. Uranium incorporation into amorphous silica. Environ. Sci. Technol. 48, 8636–8644.
Mavromatis, V., Bundeleva, I.A., Shirokova, L.S., Millo, C., Pokrovsky, O.S., Bénézeth, P., Ader, M., Oelkers, E.H., 2015. The continuous re-equilibration of carbon isotope compositions of hydrous Mg carbonates in the presence of cyanobacteria. Chem. Geol. 404, 41–51.
McCutcheon, J., Dipple, G.M., Wilson, S.A., Southam, G., 2015. Production of magnesium-rich solutions by acid leaching of chrysotile: a precursor to field-scale deployment of microbially enabled carbonate mineral precipitation. Chem. Geol. 413, 119–131.
McCutcheon, J., Wilson, S.A., Southam, G., 2016. Microbially accelerated carbonate mineral precipitation as a strategy for in situ carbon sequestration and rehabilitation of asbestos mine sites. Environ. Sci. Technol. 50, 1419–1427.
Medlin, W.L., 1961. Thermoluminescence in aragonite and magnesite. J. Phys. Chem. 65, 1172–1177.
Morgan, B., Wilson, S.A., Madsen, I.C., Gozukara, Y.M., Habsuda, J., 2015. Increased thermal stability of nesquehonite ($MgCO_3 \cdot 3H_2O$) in the presence of humidity and CO_2: implications for low-temperature CO_2 storage. Int. J. Greenh. Gas Control 39, 366–376.
Natali, C., Boschi, C., Baneschi, I., Dini, A., Chiarantini, L., 2013. Chromium mobility in Tuscan serpentinite bodies; inferences from rodingitization and carbonation. Mineral. Mag. 77, 1829.
Oelkers, E.H., Gislason, S.R., Matter, J., 2008. Mineral carbonation of CO_2. Elements 4, 333–337.
Olajire, A.A., 2013. A review of mineral carbonation technology in sequestration of CO_2. J. Pet. Sci. Eng. 109, 364–392.
Olsson, J., Stipp, S.L.S., Gislason, S.R., 2014a. Element scavenging by recently formed travertine deposits in the alkaline springs from the Oman Semail Ophiolite. Mineral. Mag. 78, 1479–1490.
Olsson, J., Stipp, S.L.S., Makovicky, E., Gislason, S.R., 2014b. Metal scavenging by calcium carbonate at the Eyjafjallajökull volcano: a carbon capture and storage analogue. Chem. Geol. 384, 135–148.
Oze, C., Bird, D.K., Fendorf, S., 2007. Genesis of hexavalent chromium from natural sources in soil and groundwater. Proc. Natl. Acad. Sci. 104, 6544–6549.
Papathanassiou, A.N., 2003. Study of the polarizable centers in single crystal dolomite ($CaMg(CO_3)_2$) rich in Fe^{3+} impurities by thermally stimulated depolarization current spectroscopy. J. Phys. Chem. Solids 64, 171–175.
Park, A.-H.A., Fan, L.-S., 2004. Mineral sequestration: physically activated dissolution of serpentine and pH swing process. Chem. Eng. Sci. 59, 5241–5247.
Park, A.-H.A., Jadhav, R., Fan, L.-S., 2003. CO_2 mineral sequestration: chemically enhanced aqueous carbonation of serpentine. Can. J. Chem. Eng. 81, 885–890.
Parkhurst, D.L., Appelo, C., 1999. User's guide to PHREEQC (Version 2): A computer program for speciation, batch-reaction, one-dimensional transport, and inverse geochemical calculations. U.S. Geological Survey, Water-Resources Investigations Report No. 99-4259.
Power, I.M., Wilson, S.A., Thom, J.M., Dipple, G.M., Gabites, J.E., Southam, G., 2009. The hydromagnesite playas of Atlin, British Columbia, Canada: a biogeochemical model for CO_2 sequestration. Chem. Geol. 260, 286–300.
Power, I.M., Dipple, G.M., Southam, G., 2010. Bioleaching of ultramafic tailings by Acidithiobacillus spp. for CO_2 sequestration. Environ. Sci. Technol. 44, 456–462.
Power, I.M., Harrison, A.L., Dipple, G.M., Wilson, S.A., Kelemen, P.B., Hitch, M., Southam, G., 2013a. Carbon mineralisation: from natural analogues to engineered systems. Rev. Mineral. Geochem. 77, 305–360.
Power, I.M., Wilson, S.A., Dipple, G.M., 2013b. Serpentinite carbonation for CO_2 sequestration. Elements 9, 115–121.
Prissok, F., Lehmann, G., 1986. An EPR study of Mn^{2+} and Fe^{3+} in dolomites. Phys. Chem. Miner. 13, 331–336.
Rai, D., Eary, L., Zachara, J., 1989. Environmental chemistry of chromium. Sci. Total Environ. 86, 15–23.
Ribet, I., Ptacek, C.J., Blowes, D.W., Jambor, J.L., 1995. The potential for metal release by reductive dissolution of weathered mine tailings. J. Contam. Hydrol. 17, 239–273.
Robie, R.A., Hemingway, B.S., 1972. The heat capacities at low-temperatures and entropies at 298.15 K of nesquehonite $MgCO_3 3H_2O$, and hydromagnesite. Ame. Mineral. 57, 1768–1781.
Rodriguez-Navarro, C., Ruiz-Agudo, E., 2012. Carbonates: an overview of recent TEM research. EMU Notes Mineral.: Miner. Nanoscale 14, 337–375.
Ryan, C.G., Siddons, D.P., Kirkham, R., Dunn, P.A., Kuczewski, A., Moorhead, G., De Geronimo, G., Paterson, D.J., de Jonge, M.D., Hough, R.M., Lintern, M.J., Howard, D.L., Kappen, P., Cleverley, J., 2010. The new maia detector system: methods for high definition trace element imaging of natural material. AIP Conf. Proc. 1221, 9–17.
Ryan, C.G., Siddons, D.P., Kirkham, R., Li, Z.Y., Jonge M.D. d. Paterson, D.J., Kuczewski, A., Howard, D.L., Dunn, P.A., Falkenberg, G., Boesenberg, U., Geronimo, G.D., Fisher, L.A., Halfpenny, A., Lintern, M.J., Lombi, E., Dyl, K.A., Jensen, M., Moorhead, G.F., Cleverley, J.S., Hough, R.M., Godel, B., Barnes, S.J., James, S.A., Spiers, K.M., Alfeld, M., Wellenreuther, G., Vukmanovic, Z., Borg, S., 2014. Maia X-ray fluorescence imaging: capturing detail in complex natural samples. J. Phys.: Conf. Ser. 499, 012002.
Ryan, C.G., 2000. Quantitative trace element imaging using PIXE and the nuclear microprobe. Int. J. Imaging Syst. Technol. 11, 219–230.
Schreier, H., 1987. Asbestos fibres introduce trace metals into streamwater and sediments. Environ. Pollut. 43, 229–242.
Schuiling, R., de Boer, P., 2013. Six commercially viable ways to remove CO_2 from the atmosphere and/or reduce CO_2 emissions. Environ. Sci. Eur. 25, 35.
Schultz, L.N., Dideriksen, K., Lakshtanov, L., Hakim, S.S., Müter, D., Haußer, F., Bechgaard, K., Stipp, S.L.S., 2014. From nanometer aggregates to micrometer crystals: insight into the coarsening mechanism of calcite. Cryst. Growth Des. 14, 552–558.
Schwertmann, U., Gasser, U., Sticher, H., 1989. Chromium-for-iron substitution in synthetic goethites. Geochim. Cosmochim. Acta 53, 1293–1297.
Seal, R.R., Piatak, N.M., Levitan, D.M., Hammarstrom, J.M., 2010. Neutral to Alkaline Mine Drainage, Carbon Sequestration, and Arsenic Release at the Abandoned Vermont Asbestos Group Mine, Belvidere Mountain, Vermont, 42. Geological Society of America Abstracts with Programs, pp. 449.
Seifritz, W., 1990. CO_2 disposal by means of silicates. Nature 345, 486.
Shan, Q., Zhang, Y., Xue, X., 2012. Removal of copper from wastewater by using the synthetic nesquehonite. Environ. Progress Sustain. Energy 32, 543–546.
Shannon, R.D., 1976. Revised effective ionic radii and systematic studies of interatomic distances in halides and chalcogenides. Acta Crystallogr. Sect. A: Cryst. Phys. Diffr. Theor. Gen. Crystallogr. 32, 751–767.
Teir, S., Kuusik, R., Fogelholm, C.-J., Zevenhoven, R., 2007a. Production of magnesium carbonates from serpentinite for long-term storage of CO_2. Int. J. Miner. Process. 85, 1–15.
Teir, S., Revitzer, H., Eloneva, S., Fogelholm, C.-J., Zevenhoven, R., 2007b. Dissolution of natural serpentinite in mineral and organic acids. Int. J. Miner. Process. 83, 36–46.
Thomas, D., Maher, K., Bird, D., Brown, G., Arnorsson, S., 2013. CO_2-rich Geothermal Areas in Iceland as Natural Analogues for Geologic Carbon Sequestration, 1. AGU Fall Meeting Abstracts, pp. 2776.
Trolard, F., Bourrie, G., Jeanroy, E., Herbillon, A.J., Martin, H., 1995. Trace metals in natural iron oxides from laterites: a study using selective kinetic extraction. Geochim. Cosmochim. Acta 59, 1285–1297.

Please cite this article in press as: Hamilton, J.L., et al., Nesquehonite sequesters transition metals and CO_2 during accelerated carbon mineralisation. Int. J. Greenhouse Gas Control (2016), http://dx.doi.org/10.1016/j.ijggc.2016.11.006

Vogel, C., Adam, C., Kappen, P., Schiller, T., Lipiec, E., McNaughton, D., 2014. Chemical state of chromium in sewage sludge ash based phosphorus-fertilisers. Chemosphere 103, 250–255.
Wilson, S.A., Raudsepp, M., Dipple, G., 2006. Verifying and quantifying carbon fixation in minerals from serpentine-rich mine tailings using the Rietveld method with X-ray powder diffraction data. Am. Mineral. 91, 1331–1341.
Wilson, S.A., Dipple, G.M., Power, I.M., Thom, J.M., Anderson, R.G., Raudsepp, M., Gabites, J.E., Southam, G., 2009. Carbon dioxide fixation within mine wastes of ultramafic-hosted ore deposits: examples from the Clinton Creek and Cassiar Chrysotile deposits, Canada. Econ. Geol. 104, 95–112.
World Health Organisation, 2011. Guidelines for Drinking-water Quality, 4th edition. WHO, Geneva.
Wunsch, A., Navarre-Sitchler, A.K., Moore, J., Ricko, A., McCray, J.E., 2013. Metal release from dolomites at high partial-pressures of CO_2. Appl. Geochem. 38, 33–47.
Zachara, J.M., Cowan, C.E., Resch, C.T., 1991. Sorption of divalent metals on calcite. Geochim. Cosmochim. Acta 55, 1549–1562.

Please cite this article in press as: Hamilton, J.L., et al., Nesquehonite sequesters transition metals and CO_2 during accelerated carbon mineralisation. Int. J. Greenhouse Gas Control (2016), http://dx.doi.org/10.1016/j.ijggc.2016.11.006